

Motion of vacancy islands on an anisotropic surface: Theory and kinetic Monte Carlo simulations

Karina Morgenstern,^{1,2} Erik Lægsgaard,² and Flemming Besenbacher²

¹*Institut für Experimentalphysik, FB Physik, Freie Universität Berlin, Arnimallee 14, D-14195 Berlin, Germany*

²*CAMP and Institute of Physics and Astronomy, University of Aarhus, DK-8000 Aarhus C, Denmark*

(Received 21 November 2001; published 12 September 2002)

Recently, scanning tunneling microscopy results on the Brownian motion of two-dimensional vacancy islands on Ag(110) were presented. While the detachment of adatoms from the island and their diffusion on the terrace was permitted in the temperature range between 180 K and 220 K, the periphery diffusion of single adatoms was prohibited. The Brownian motion of the islands was found to follow a simple scaling law with terrace diffusion being the rate-limiting process. The scaling of the experimental results was confirmed by kinetic Monte Carlo (kMC) simulations. Here, we elaborate on the results and especially present a detailed derivation of the equation that relates the diffusivity of an anisotropic island to its size. Further details and results on the kMC simulations will be presented as well. Our results shed light on the recently discussed issue of attempt frequencies for surface diffusion. In this specific case of an anisotropic surface, we obtain prefactor ratios for exchange and hopping mechanisms.

DOI: 10.1103/PhysRevB.66.115408

PACS number(s): 61.43.Bn, 68.35.Fx, 36.40.Sx, 05.40.Jc

I. INTRODUCTION

The motion of two-dimensional islands has received much attention in recent years because of its relevance to crystal growth. An island migrates since fluctuations in its shape cause random shifts of its center of mass. The mechanisms for mass transport for small islands (≈ 10 – 1000 atoms) on metal surfaces are considered to be (i) periphery diffusion, where adatoms hop along the step edge but do not detach from it, (ii) correlated terrace diffusion, where adatoms detach from the step edges, diffuse on the terraces, and reattach to the step edge, and (iii) uncorrelated terrace diffusion, also called the evaporation/recondensation mechanism, where an additional barrier for adatoms to attach to a step edge suppresses correlation. In the case of metal surfaces this prerequisite for the third mechanism does not exist.^{1,2}

Substantial effort, both theoretically^{1–4} and experimentally,^{5–7} has been devoted to the investigation of whether the island diffusion can be understood in terms of simple scaling laws.⁸ It has been argued both from macroscopic theories¹ and from simple scaling relations^{5,8} that the diffusion coefficient D of an island should depend on its diameter d via

$$D \propto d^{-\beta}. \quad (1)$$

The temperature-independent exponent β depends on the rate-limiting mass transport mechanism. Exponents of 3 and 2 have been predicted for periphery diffusion and correlated terrace diffusion, respectively.^{1,5,8}

Experimentally, the Brownian motion of both vacancy and adatom islands has mainly been studied on the *isotropic* surfaces of Ag and Cu.^{5–7} On fcc(111) and fcc(100) surfaces, the energy barrier for adatom periphery diffusion is substantially lower than the detachment energy of atoms from the island edges. This finding is obtained from ripening experiments where detachment rates are measured.⁹ The observed island displacements are thus caused by periphery diffusion

of the adatoms. The experimental results^{6,7} do not, however, fulfill the simple universal scaling relation in Eq. (1) with an integer value for β . The same applies for the kinetic Monte Carlo (kMC) simulations.^{2,3} Rather noninteger and nonuniversal β values between 1.5 and 2.5 were found depending on both temperature and substrate material. Only very recently, kMC simulations based on a bond-counting ansatz resulted in a scaling law relation with the exponent 2 on a square lattice at least for low temperatures.¹⁰ In the case of periphery diffusion, the deviation from the predicted universal scaling with integer β exponents seems to be caused by defects hindering the periphery diffusion, e.g., kinks, and the difficulty of core breakup.^{3,4,7,11}

We have recently studied a relevant model system,¹² the diffusion of vacancy islands on an anisotropic Ag(110) surface, where the terrace diffusion is the rate-limiting, atomic-scale diffusion mechanism. We anticipate Eq. (1) to hold, since no obstacles should impede terrace diffusion. For the motion of vacancy islands in the $\langle 110 \rangle$ direction our scanning tunneling microscopy (STM) results clearly revealed that a simple universal scaling is obeyed with an integer exponent $\beta=2$ and an activation energy for the diffusivity of $E_D = (0.41 \pm 0.06)$ eV.¹²

In this paper, we present the details on how Eq. (1) can be derived for terrace diffusion on an anisotropic surface. We show that this equation is fulfilled both in experiments and in kMC simulations. The kMC simulation reproduces details of the experimental results. In particular, the simple scaling law derived theoretically exists in kMC simulations for the motion of vacancy islands in the $\langle 110 \rangle$ direction on the Ag(110) surface independent of relative prefactors for the hopping and exchange mechanism ν_{ex}/ν_h . From the kMC simulations we derive an upper limit of $\nu_{ex}/\nu_h < 5$.

II. EXPERIMENT

The STM experiments have been performed in a UHV system equipped with a home-built, fast-scanning, variable-

temperature STM as well as standard facilities for sample preparation and characterization.¹³ The anisotropic Ag(110) surface is prepared by several sputtering (1 keV Ne⁺) and annealing cycles (623 K) below the roughening temperature followed by a slow cool down (10 K/min). This procedure results in a clean, well-ordered Ag(110) surface. Vacancy islands are created by 1-keV Ne⁺ sputtering at 180–210 K for 1–5 s. At these temperatures the single vacancies are sufficiently mobile to agglomerate into vacancy islands of monatomic depth.

The mobility of the vacancy islands is studied in so-called STM movies, i.e., series of time-lapsed STM images¹³ (256×256 pixels) recorded at time intervals from ≈ 6 s to ≈ 20 s. Special care was taken to ensure that the island mobility data was not influenced by the STM imaging process.⁹

The kMC simulations have been performed on a grid of 150×40 atoms. The grid is sufficiently large that a vacancy will not encounter a border of the grid in any of the simulations. The program is written in DELPHI5 and runs on a PC with the standard random generator of Borland Delphi, which we have thoroughly checked for correlations. We define one step in this standard kMC simulation as one million cycles. In each cycle an atom and a direction are chosen randomly and the atom is moved into this direction with a probability determined by the presence or absence of its nearest and next-nearest neighbors. The probabilities P are calculated based on the energies E listed in Table I according to $P = \nu e^{E/kT}$, assuming different prefactors for the hopping motion along the atomic rows ν_h and for the exchange motion perpendicular to them, ν_{ex} . For all hopping processes and for all exchange processes, however, a single prefactor is assumed. These are scaled to $\nu_h = e^{-E_D/kT}$ with $E_D = 0.28$ eV, the diffusion energy of an adatom on the terrace (see Table I). Only motions between neighboring lattice sites are included, i.e., no long jumps are allowed.

The initial configuration consists of a rectangular island with a given aspect ratio. The island is placed in the center of the grid and several MC steps (the number of steps depending on temperature) are run until an equilibrium aspect ratio is reached. In the temperature range investigated equilibration of the adatom concentration within the island is always much faster than equilibration of the island shape. A MC run is started and the island's center-of-mass position and its aspect ratio are recorded at regular time intervals. The number of Monto Carlo steps between the recording of the positions of the island depends on temperature and is chosen such that the center-of-mass displacement of the island is on average at least half an atomic distance in the $\langle 110 \rangle$ direction. One kMC run consists of 100 island positions. The kMC results presented in this paper are based on a minimum of 10 runs for each set of initial parameters.

III. RESULTS AND DISCUSSION

A. Scaling law for an anisotropic surface

In the following, we will derive the simple scaling relation Eq. (1) for terrace diffusion on an anisotropic surface.

TABLE I. Energies (in eV) used in the kMC calculations. Energies were calculated with molecular dynamics with the program artwork based on effective-medium potentials (Ref. 18). NN is the number of nearest neighbors, i.e., neighbors in the $\langle 110 \rangle$ direction. NNN is the number of next-nearest neighbors, i.e., the neighbors in the $\langle 001 \rangle$ direction. NN/NNN_{pre} before the motion, NN/NNN_{post} after the motion. All processes in the $\langle 001 \rangle$ direction are exchange processes.

NN _{pre}	→	NN _{post}	NNN _{pre}	→	NNN _{post}	$\langle 110 \rangle$	$\langle 001 \rangle$
0	-	0	2	-	2	0.21	
0	-	0/1	0	-	0/1/2	0.28	
0	-	0/1	1	-	1/2	0.28	
0	-	0/1	2	-	2	0.28	
0	-	0/1	1	-	0	0.30	
0	-	0/1	2	-	1	0.30	
0	-	0/1	2	-	0	0.32	
0	-	0/1/2	0	-	0/1		0.39
1	-	1/2	0	-	0/1		0.39
2	-	2	0	-	0/1		0.39
0	-	0/1/2	1	-	0/1		0.41
1	-	1/2	1	-	0/1	0.41	
2	-	2	1	-	0/1	0.41	
1	-	0/1	0	-	0/1/2	0.45	
1	-	0/1	1	-	1/2	0.45	
1	-	0/1	2	-	2	0.45	
1	-	0/1	1	-	0	0.47	
1	-	0/1	2	-	1	0.47	
1	-	0/1	2	-	0	0.49	
1	-	0	0	-	0/1		0.56
2	-	1	0	-	0/1		0.56
1	-	0	0	-	0/1		0.58
2	-	1	0	-	0/1		0.56

To derive this equation for an anisotropic surface, we closely follow the deduction for the isotropic case presented in Ref. 5.

Let us consider an island of length l and width w as depicted in Fig. 1. For the island to move a distance δl in the indicated x direction, all material in the dark gray region has to be moved into the light gray region. According to Pimpinelli *et al.*¹⁴ the relation between the shaded area $w \delta l$ and the number $N(\delta t)$ of atoms that move during the time δt is given by

$$w \delta l n_S = \sqrt{N(\delta t)} \quad (2)$$

with n_S being the atomic density in the surface layer. This equation accounts for the fact that only some of the detaching atoms will reach the opposite side of the vacancy island. Most of the atoms will reattach to the same side causing no center-of-mass motion of the island as a whole. The number of atoms that move during the time interval δt is given by

$$N(\delta t) = N_0 \delta t / \tau, \quad (3)$$

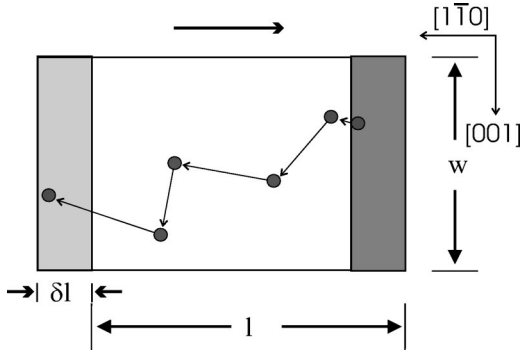


FIG. 1. Sketch of the geometry of an anisotropic island moving by terrace diffusion of the adatoms.

where τ is the mean travel time for an adatom to diffuse from one edge to the other (in x direction). The number of adatoms N_0 which move at a certain time t is given by

$$N_0 \propto \rho_S w l \quad (4)$$

with ρ_S being the equilibrium concentration of surface adatoms on the surface. From the Einstein relation describing the random motion of an atom in the x direction we obtain

$$\tau \propto l^2 / D_S, \quad (5)$$

where D_S is the diffusivity of atoms for terrace diffusion. From Eqs. (2)–(5) we obtain

$$\delta l^2 \propto \frac{D_S \rho_S}{l w n_s^2} \delta t. \quad (6)$$

If we compare this to the Einstein relation for a nanoscopic object with diffusivity D ,

$$\langle (\Delta l)^2 \rangle = 2D \Delta t, \quad (7)$$

it becomes evident that Eq. (6) describes the random motion of a vacancy island in the x direction with the diffusivity,

$$D \propto \frac{1}{l w} = (\sqrt{A})^{-2}. \quad (8)$$

This simple derivation shows that the diffusivity of the islands on an anisotropic surface scales with the square root of the island area A with a scaling exponent of -2 .

Equation (5) is valid independently of the amount of motion in the (independent) y direction. This equation, however, requires an unhindered random motion of the single adatoms. This is the equation that is not fulfilled in the case of periphery diffusion on the isotropic surfaces discussed above leading to deviations from the simple scaling law behavior.

B. Experiments

Figure 2(a) shows the first and the last image from a STM movie recorded at 213 K over 10 min. The displacement of the vacancy islands (black) along the close-packed rows ($\langle 110 \rangle$, x direction) is several nanometers on the time scale of minutes.

Figure 2(b) displays the relative motion of the center of mass of two vacancy islands at 202 K. We always record the relative motion of two islands to avoid errors on the measured island diffusivities due to a possible thermal drift. Parallel to the close-packed rows, the erratic motion extends over about eight atomic distances within 1 h. Smaller islands of about half the area move about 14 atomic distances in the x direction in the same time and at the same temperature [Fig. 2(c)]. The motion perpendicular to the close-packed rows ($\langle 001 \rangle$, y direction) is for the smaller islands less than two atomic distances in both cases. This behavior indicates qualitatively that the motion parallel to the close-packed rows is random, also called Brownian, whereas the motion perpendicular to the rows is not Brownian. Quantitatively, a Brownian motion must follow the Einstein relation [Eq. (7)].

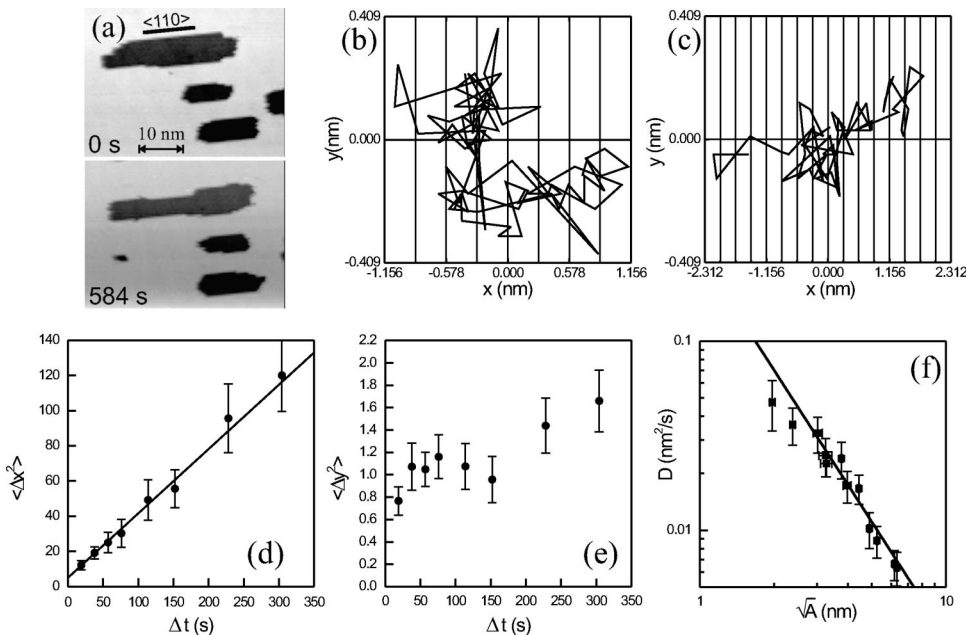


FIG. 2. Experimental results: (a) first and last STM image of a movie taken at 213 K over a time interval of 10 min, $U = -0.5$ V, $I = 0.04$ nA; (b) and (c) relative displacement of the center of mass of two islands at 202 K, $\Delta t = 19$ s. The grid represents atomic surface positions of the adatoms in the surface layer. (b) $A_1 = 1.35$ nm² and $A_2 = 1.67$ nm²; (c) $A_1 = 0.71$ nm² and $A_2 = 0.96$ nm² (d) and (e) relative mean-square displacement versus elapsed time Δt for relative motion in (c); (e) diffusivity versus island size at 194 K.

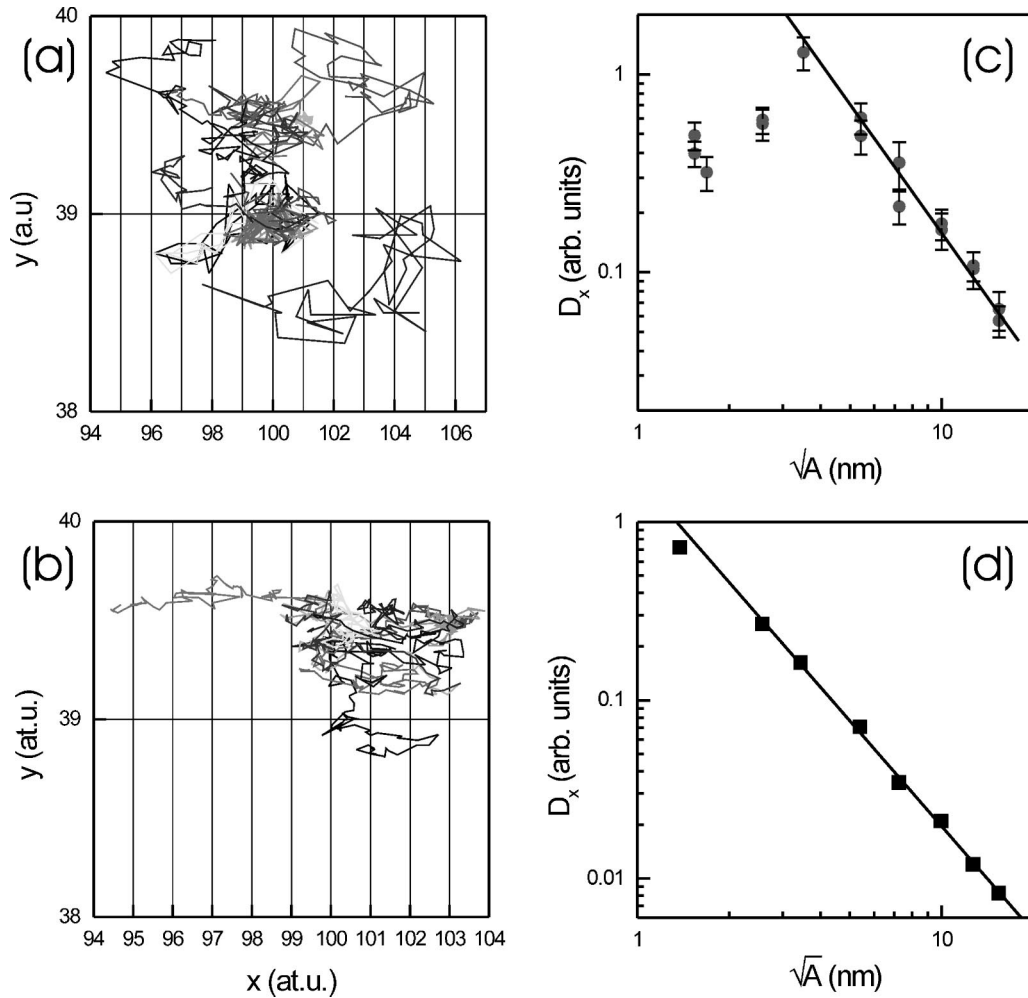


FIG. 3. Results of kMC simulations: (a) and (b) Trajectories of 10 vacancy islands (different shades of gray represent different MC runs) (a) $T=270$ K, $A=245$ at, $v_{ex}/v_h=1$, $\Delta t=1\,000\,000$ MC; (b) $T=300$ K, $A=245$ at, $v_{ex}/v_h=1$, $\Delta t=50\,000$ MC; (c)(d) Dependence of diffusivity on island size at (c) 270 K and (d) 300 K, respectively.

Indeed, Figs. 2(d) and 2(e) demonstrate that for the motion in x direction the relative mean-square displacement $\langle(\Delta x)^2\rangle$ is proportional to Δt , whereas for $\langle(\Delta y)^2\rangle$ this relation is not fulfilled.

To analyze the experimentally measured Brownian motion parallel to the rows, we determine the island diffusivity D via $D=\langle(\Delta x)^2\rangle/4\Delta t$ with Δt being the time elapsed between consecutive STM images.⁵ Figure 2(f) displays a double-logarithmic plot D versus \sqrt{A} for 194 K. The slope of the linear fit to the STM data is very close to the integer value of 2, consistent with the scaling theory [according to Eq. (8)].

C. Kinetic Monte Carlo simulation

Figure 3 displays results from the kMC simulations at 270 K and 300 K. In order to have comparable motion at 270 K and 300 K the time constant for 270 K is 20 times as many MC cycles as the one at 300 K. The trajectories of simulated vacancy islands [Figs. 3(a) and 3(b)] show qualitative similarities to the experimental data [Figs. 2(b) and 2(c)]. The motion parallel to the close-packed rows is random while the

perpendicular motion is limited to less than two atomic distances. With the same analysis procedure as utilized on the experimental data the diffusivity is determined from the mean-square displacement, plotted as a function of the square root of the island area \sqrt{A} [Figs. 3(c) and 3(d)]. Again, the scaling of the diffusivity $D(\sqrt{A})$ is consistent with Eq. (8) with a scaling exponent close to 2.

For islands smaller than $\sqrt{A}\approx 2.0$ nm, i.e., $A\approx 35$ atoms, we find that the kMC simulations deviate from this scaling behavior. This is hardly surprising. An island of this size with an equilibrium aspect ratio of ≈ 3 (Ref. 15) has a width of only three vacancies. An atom diffusing within such a small vacancy island will therefore very often encounter the periphery of the island (with every second motion in the y direction). This hampers unhindered terrace diffusion and Eq. (5) is no longer fulfilled. Indeed, the much stronger fluctuations of the aspect ratio suggest a different process to be dominant in this case. A close inspection of the experimental data shown in Fig. 2(f) reveals a deviation from the scaling law for smaller islands as well.

Molecular-dynamics simulations showed¹⁵ that independent of the number of nearest and next-nearest neighbors, the

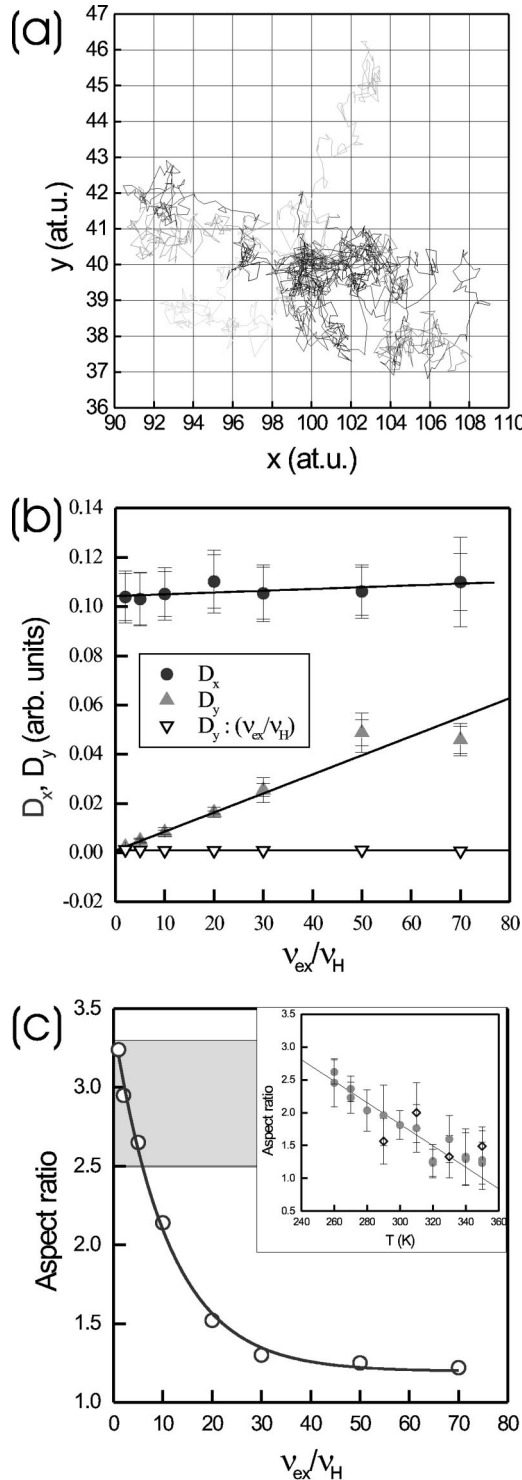


FIG. 4. Test of relative attempt frequency ($T=300$ K, $A=165$ at ≈ 19 nm²): (a) Trajectories of 10 vacancy islands (different shades of gray represent different MC runs), $v_{ex}/v_h=70$, $\Delta t=50\,000$ MC; (b) Dependence of diffusivity on relative attempt frequency, v_{ex}/v_h . D_x (circles), D_y (up triangles), and $D_y/(v_{ex}/v_h)$ (down triangles) with linear fits. (c) Dependence of aspect ratio on relative attempt frequency. Shaded area represents experimental value (Ref. 15). Fit is exponential. Inset: Dependence of aspect ratio on temperature for an island of 150 atoms and a relative attempt frequency of 1.

atom motion follows a different process along and perpendicular to the close-packed rows. Motion in the x direction proceeds via the hopping mechanism, while the perpendicular motion proceeds via the exchange mechanism. The latter mechanism requires the correlated motion of two atoms. It has recently been suggested that exchange processes have an attempt frequency ν_{ex} that is more than one order of magnitude larger than the ordinary hopping attempt frequencies for surface diffusion ν_h .¹⁶ An enhanced prefactor ratio, $\nu_{ex}/\nu_h=20$, has been calculated for the case of Cu(100). It has been suggested that this may be a general phenomenon valid also for exchange processes for other surfaces. We have therefore investigated the influence of the attempt frequencies on the island's diffusivity in the kMC simulations by varying the prefactor ratio ν_{ex}/ν_h from 1 to 70. The enhanced prefactor ratio leads to an enhanced island motion perpendicular to the close-packed rows [Fig. 4(a)]. The diffusivity in the y direction shows a linear dependence on ν_{ex}/ν_h [Fig. 4(b)]. In contrast, the variation of ν_{ex}/ν_h does not have any influence on the diffusivity for the motion of the island in the x direction [Fig. 4(b)].

The equilibrium aspect ratio for the islands also changes with ν_{ex}/ν_h [Fig. 4(c)]. For the case of a vacancy island of 165 vacancies at 300 K the aspect ratios drop exponentially from 3.24 to 1.22 going from $\nu_{ex}/\nu_h=1$ to $\nu_{ex}/\nu_h=70$. Furthermore, the simulation of the change in aspect ratio by temperature shows that the aspect ratio *increases* with decreasing temperature [Fig. 4(c), inset]. Experimentally, we determined the equilibrium aspect ratio at 250 K to be 2.9 ± 0.4 .¹⁵ This deviates from the aspect ratio for $\nu_{ex}/\nu_h=20$. Instead, it suggests that the prefactors differ by less than a factor of 5. However, to finally decide this issue, calculations of the different prefactors similar to the calculations done for Cu(100) (Ref. 16) are required.

IV. CONCLUSION

We have presented kinetic Monte Carlo simulations for vacancy island diffusion on Ag(110). These demonstrate that the Brownian motion of vacancy islands on the Ag(110) surface parallel to the close-packed rows follows a simple universal scaling law. The scaling exponent of 2 is consistent with the fact that terrace diffusion is the rate-limiting step independent of the prefactor for exchange motion perpendicular to the close-packed rows. The diffusivity perpendicular to the rows depends linearly on the prefactor ratio. A shape analysis sheds light on the much discussed prefactors¹⁷ and suggests that the prefactor ratio is certainly smaller than 5.

ACKNOWLEDGMENT

We acknowledge the financial support by the Danish National Research Foundation through the Center for Atomic-scale Materials Physics (CAMP) and from the VELUX and Knud Højgaard's Foundations.

- ¹C. DeW. Van Siclen, Phys. Rev. Lett. **75**, 1574 (1995); S.V. Khare, N.C. Bartelt, and T.L. Einstein, *ibid.* **75**, 2148 (1995); J.M. Soler, Phys. Rev. B **53**, R10 540 (1996); S.V. Khare and T.L. Einstein, *ibid.* **54**, 11 752 (1996); **57**, 4782 (1998).
- ²A.F. Voter, Phys. Rev. B **34**, 6819 (1986); D.S. Scholl and R.T. Skodje, Phys. Rev. Lett. **75**, 3158 (1995); U. Kürpick, P. Kürpick, and T.S. Rahman, Surf. Sci. **383**, L713 (1999); J. Heinonen, I. Koponen, J. Merikoski, and T. Ala-Nissila, Phys. Rev. Lett. **82**, 2733 (1999); S. Pal and K.A. Fichtorn, Phys. Rev. B **60**, 7804 (1999).
- ³A. Bogicevic, S. Liu, J. Jacobsen, B. Lundqvist, and H. Metiu, Phys. Rev. B **57**, R9459 (1998).
- ⁴G. Mills, T.R. Mattsson, L. Mollnitz, and H. Metiu, J. Chem. Phys. **111**, 8639 (1999).
- ⁵K. Morgenstern, G. Rosenfeld, B. Poelsema, and G. Comsa, Phys. Rev. Lett. **74**, 2058 (1995).
- ⁶J.-M. Wen, S.-L. Chang, J.W. Burnett, J.W. Evans, and P.A. Thiel, Phys. Rev. Lett. **73**, 2591 (1994); J.-M. Wen, J.W. Evans, M.C. Bartelt, J.W. Burnett, and P.A. Thiel, *ibid.* **76**, 652 (1996); A.M. Cadilhe, C.R. Stoldt, C.J. Jenks, P.A. Thiel, and J.W. Evans, Phys. Rev. B **61**, 4910 (2000); W.W. Pai, A.K. Swan, Z. Zhang, and J.F. Wendelken, Phys. Rev. Lett. **79**, 3210 (1997).
- ⁷D. Schlößer, K. Morgenstern, L.K. Verheij, G. Rosenfeld, F. Besenbacher, and G. Comsa, Surf. Sci. **465**, 19 (2000).
- ⁸K. Binder and D. Stauffer, Phys. Rev. Lett. **33**, 1006 (1974); M. Rao, M.H. Kalos, J.L. Lebowitz, and J. Marro, Phys. Rev. B **13**, 4328 (1976).
- ⁹K. Morgenstern, G. Rosenfeld, E. Laegsgaard, F. Besenbacher, and G. Comsa, Phys. Rev. Lett. **80**, 556 (1998); K. Morgenstern, G. Rosenfeld, and G. Comsa, Surf. Sci. **441**, 289 (1999).
- ¹⁰T. Müller and W. Selke, Eur. Phys. J. B **10**, 549 (1999).
- ¹¹J.F. Wendelken, A.K. Swan, W.-W. Pai, and J.-K. Zuo, in *Morphological Organization in Epitaxial Growth and Removal*, edited by Z. Zhang and M. Lagally (World Scientific, Singapore, 1998).
- ¹²K. Morgenstern, E. Laegsgaard, and F. Besenbacher, Phys. Rev. Lett. **86**, 5739 (2001).
- ¹³F. Besenbacher, Rep. Prog. Phys. **59**, 1737 (1996).
- ¹⁴A. Pimpinelli, J. Villain, D.E. Wolf, J.J. Metois, J.C. Heyraud, I. Elkinani, and G. Uimin, Surf. Sci. **295**, 143 (1993).
- ¹⁵K. Morgenstern, E. Laegsgaard, I. Stensgaard, and F. Besenbacher, Phys. Rev. Lett. **83**, 1613 (1999).
- ¹⁶G. Boisvert, N. Mousseau, and L.J. Lewis, Phys. Rev. B **58**, 12667 (1998).
- ¹⁷K.R. Roos and M.C. Tringides, Phys. Rev. Lett. **85**, 1480 (2000); K. Morgenstern and F. Besenbacher, Phys. Rev. Lett. **87**, 149603 (2001); *Collective Diffusion : Correlation Effects and Adatom Interactions*, edited by M. Tringides and Z. Chvoj (Kluwer Academic Publishers, Dordrecht, 2001).
- ¹⁸P. Stoltze, J. Phys.: Condens. Matter **6**, 9495 (1994); J.K. Nørskov, K.W. Jacobsen, P. Stoltze, and L.B. Hansen, Surf. Sci. **283**, 277 (1993).